Azerbaijani Astronomical Journal AAJ **21(1)**, 62–67 (2026) Accepted 31 May 2026 https://doi.org/10.59849/2078-4163.2026.1.62

JUPITER IN THE 890 NM METHANE ABSORPTION BAND: A RESEARCH REVIEW

A. M. Karimov[1]★, S. K. Salamakhin[1]
[1] *V. G. Fesenkov Astrophysical Institute, Observatory 23, 050020 Almaty, Kazakhstan*

Last updated 2026 April 19; in original form 2026 May 28

ABSTRACT
Jupiter's atmosphere is a complex dynamic system with a multilayered cloud structure and intense circulation processes. Near-infrared observations, particularly in the methane absorption band around 890 nm, provide a powerful diagnostic tool for the upper atmosphere. This paper presents a comprehensive analysis of observational data in the 890 nm band, including a comparison with brightness temperatures in the far-infrared and microwave ranges. Observations show that the central depth of the methane absorption band closely correlates with stratospheric temperatures at pressure levels of 3.5–8.6 mbar. The largest deviations are observed in the Great Red Spot (GRS) region, reflecting its unique vertical and dynamic structure. High latitudes and equatorial anticyclonic formations, as well as variations in aerosol optical depth, contribute to the observed photometric contrasts. The results demonstrate that the 890 nm methane absorption band is a sensitive tool for studying stratospheric haze and upper tropospheric dynamics, providing important constraints for atmospheric modeling and interpretation of high-resolution ground-based and space-based observations.

Key words: Jupiter – atmosphere – methane absorption – near infrared – aerosols – Great Red Spot – stratosphere – troposphere – planetary spectroscopy.

1 INTRODUCTION

Jupiter's atmosphere is a complex dynamic system with a multilayered cloud structure and intense circulation processes. One of the key methods for diagnosing its upper layers is observations in the near-infrared spectral region, in particular in the strong methane absorption band around 890 nm. Diffuse reflectance levels of solar radiation in this spectral region correspond to pressures from 5–70 mbar in the polar regions to 100–200 mbar in the equatorial zone (Morales-Juberıas et al. 2003; Banfield et al. 1998). This pressure range reflects the altitudes at which the observed radiation is formed and allows this band to be used as a diagnostic tool for studying the upper troposphere and lower stratosphere of the planet. This method allows one to study the properties of aerosols, the thermal structure, and the dynamics of high atmospheric layers inaccessible to observations in the visible range. This is due to the fact that in the region of strong methane absorption, the contribution of deeper atmospheric layers is significantly weakened, and the recorded radiation is formed predominantly at high altitudes.

Methane absorption band and a brief analysis of the absorption in this band compared to brightness temperatures in the far infrared and microwave ranges. This comparison is of particular interest because it allows us to establish a possible relationship between the radiative characteristics of the atmosphere and its thermal structure at different altitudes. Analysis of such relationships is important for a deeper understanding of the physical processes that determine the vertical and latitudinal structure of Jupiter's atmosphere, as well as for refining existing atmospheric models of the planet.

2 A REVIEW OF PUBLISHED FILTER OBSERVATIONS OF JUPITER IN THE METHANE ABSORPTION BAND OF 890 NM

Images obtained at 890 nm reflect changes in high clouds and the upper haze layer at a pressure level of 150–200 mbar (Morales-Juberıas et al. 2003). This means that observations in this spectral region are predominantly sensitive to the upper troposphere and lower stratosphere, where the main aerosol structures are formed. In polar regions, data at 889 nm are an indicator of the highest formations of stratospheric aerosol, concentrated between the levels of 5 and 70 mbar (Banfield et al. 1998). Thus, observations in this band make it possible to reveal the distribution of high-lying aerosol haze, especially in regions characterized by intense stratospheric dynamics. High cloud tops and thick clouds at the tops of plumes explain the anomalously low equivalent width of the 890 nm methane absorption band (Banfield et al.

★ E-mail: karalik0@mail.ru

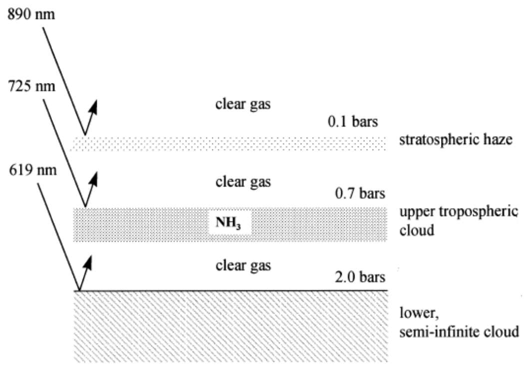

Figure 1. Model of Jupiter's atmosphere. Different layers of the atmosphere are sensitive to radiation at different wavelengths (Bellini et al. 1998).

1998). This is due to the fact that an increase in the height of cloud tops reduces the effective path length of the absorbing gas, which leads to a weakening of the observed absorption.

The stratification of Jupiter's atmosphere, not only meridionally but also vertically, leads to significant differences in observational data obtained at wavelengths of 619 and 890 nm, as demonstrated by West et al. in their analysis of data for 619, 725, and 890 nm (West et al. 1986). These differences are due to the fact that each of these wavelengths is characterized by different radiation penetration depths and, therefore, is sensitive to different atmospheric altitudes. As a result, observations at different wavelengths provide information on the vertical structure of the atmosphere and the distribution of aerosol and gaseous components. In the work of Bellini et al. (1998) a diagram of the penetration of radiation of different wavelengths with subsequent reflection from different layers of the atmosphere of Jupiter is presented (Bellini et al. 1998). This diagram is shown in Fig. 1. The presented model allows us to clearly illustrate which atmospheric layers make the main contribution to the formation of the observed radiation at different wavelengths. As can be seen from Fig. 1, this model consists of a lower semi-infinite cloud with an upper boundary at a pressure of about 2.0 bar, an upper tropospheric ammonia cloud with a base at 0.7 bar, and stratospheric haze above them at a pressure of about 0.1 bar. Pure gas fills the space between all layers. This multilayered structure of the atmosphere determines the complex nature of the interaction of radiation with cloud and gas components. While the 890 nm wavelength is sensitive to stratospheric haze and gas above the upper clouds, the 725 nm wavelength is sensitive to the upper layers of ammonia clouds and everything located above them, and the 619 nm wavelength also captures gas between the upper and lower clouds at a level of 2 bar Bellini et al. (1998), and possibly penetrates deeper - to the third ammonia-water cloud layer at a level of 4-5 bar. Thus, a combination of observations at different wavelengths allows for multi-level diagnostics of Jupiter's atmosphere. According to other authors, the atmospheric level sensitive to the 890 nm band differs somewhat. Hill et al. believe that it is at a level of approximately 0.6 bar (Hill et al. 2023). Wong et al. establish it at a level of 0.3-0.5 bar (Wong et al. 2023). Differences in these estimates may be due to the use of different atmospheric models, as well as the peculiarities of the processing of observational data. Apparently, the latter estimate is the most probable, since it is confirmed by the great external similarity of the zonal-striped structure of Jupiter's atmosphere in images in the continuous spectrum (IR) and in the CH_4 absorption band of 890 nm (Figure 2). This similarity indicates that the bulk of reflected radiation in these spectral regions is generated at similar atmospheric altitudes. The observed differences can be explained by variations in the thickness of the purely gaseous atmosphere above the belts and zones, or by variations in the density and scattering properties of the upper cloud layers, to which the center of the deep 890 nm CH_4 absorption band is very sensitive. Thus, the observed variations reflect real physical differences in the structure of the planet's atmosphere. Wallace and Smith (1977) modeled near-infrared spectra and center-to-limb oscillation observations for the 0.49 and 0.89 μm bands using newly measured methane absorption coefficients. This suggested that the cloud-top pressure of 200–300 mbar is too high to correspond to the condensation level of ammonia ice (West et al. 1986). This points to the need to refine models of Jupiter's cloud structure and the possible presence of additional aerosol chromophore components formed by photochemical reactions.

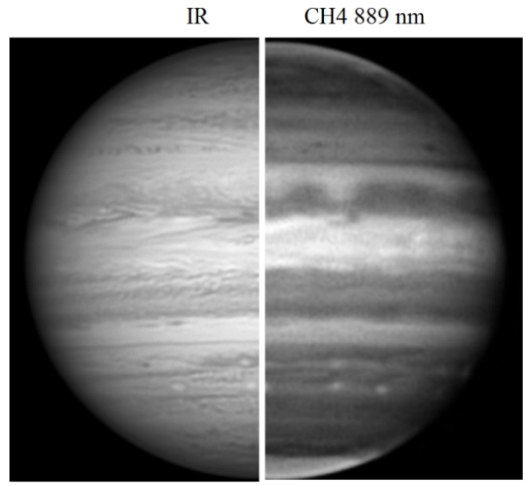

Figure 2. Jupiter's appearance in the infrared (IR) continuum (left) and in the methane absorption band at 889 nm (right), based on images obtained by Christopher Go on May 24, 2018 (`https://alpo-j.sakura.ne.jp/kk18/j180524z.htm`).

In the late 1970s and early 1980s, West and others interpreted the band/continuum ratios and center-to-limb brightness variations using high-signal-to-noise CCD images in the 0.619, 0.725, and 0.89 μm bands. They also found suitable conditions for two types of models: one with a gas layer above a semi-infinite homogeneous scattering/absorbing layer, and the other with two discrete, physically thin tropospheric clouds plus a thin stratospheric haze (West et al. 1986). Both models explain the observed photometric characteristics of the planet's disk and confirm the complex vertical structure of the atmosphere.

Similar work was conducted by Vdovichenko and Teifel and colleagues on spectral observations in the 600-1000 nm range (Atai et al. 2022; Vdovichenko et al. 2017; Teifel et al. 2017; Vdovichenko et al. 2016, 2014, 2015; Teifel et al. 2018). Overall, the difference in absorption in the 619 and 890 nm bands indicates a difference in the thermal balance of Jupiter's troposphere and stratosphere. This is due to the fact that these spectral regions are sensitive to different atmospheric altitudes, characterized by different thermodynamic conditions.

3 ABSORPTION COEFFICIENTS

Owen and Manson determined the absorption coefficients for the 890 nm band using the Beer–Lambert law:

$$I = I_0 e^{-kx} \quad (1)$$

Here, I_0 is the solar energy flux at the top of the atmosphere, e is the base of the natural logarithm, k is the absorption coefficient, and x is the equivalent path length. The following values of the absorbing layer per unit pressure (equivalent path) were used: 60 ± 30 m/atm for the north polar region, 40 m/atm for the equatorial zone (EZ), and 34 m/atm for the Great Red Spot (GRS) (Owen & Mason 1969). These values indicate significant differences in the optical properties of the atmosphere at different latitudes of the planet.

The basic information on the absorption coefficients in the 890 nm methane band was obtained from a 1994 study by Karkoschka (Karkoschka 1994). It was noted that "the narrowing of methane absorption bands toward lower temperatures leads to strong temperature dependencies at the band edges, where the methane spectrum exhibits a steep gradient." This implies that the spectral characteristics of methane vary significantly with environmental temperature, which is particularly important when interpreting observations of giant planet atmospheres. The steepest linear gradient at wavelengths shorter than 1000 nm occurs near 880 nm. At this wavelength, the absorption coefficient of methane decreases by approximately a factor of 4 when transitioning from room temperature to the temperature of Jupiter's atmosphere. Such a change indicates a high sensitivity of methane spectral characteristics to temperature conditions. Additional steep gradients are observed near 980 nm, where the decrease is approximately threefold, and near 905 nm, where it is approximately twofold. At these wavelengths, the temperature dependence is sufficiently strong that the temperature differences between the atmospheres of Jupiter and Saturn become significant (Karkoschka 1994).At 880 nm, the absorption coefficient of methane is approximately 20% higher for Jupiter than for Saturn. Although this difference is notable, it is significantly smaller than the variation factor of 4. Therefore, temperature effects must be taken into account in the quantitative analysis of observational data.Once methane absorption at these wavelengths is definitively established by laboratory measurements, these wavelengths may be able to be used as an effective thermometric indicator of Jupiter's atmosphere (Karkoschka 1994). This opens the prospect of using spectral observations of methane to remotely determine the atmospheric temperatures of giant planets.

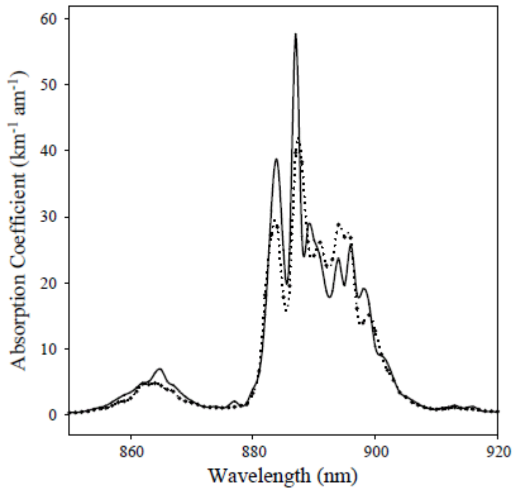

Figure 3. Absorption coefficients (averaged over a 1 nm interval) for methane at 77 K compared with Karkoschka values (Teifel et al. 2017).

A comparison of laboratory data with the results of Karkoschka is presented in the study by O'Brien and Cao (2002), where the distribution of the methane absorption coefficient in the 890 nm band at a temperature of 77 K is shown graphically (O'Brien & Cao 2002). Figure 3 from that paper (O'Brien & Cao 2002) is presented below. The obtained results serve as an important reference for interpreting observations of the atmospheres of Jupiter and Saturn, whose temperatures are close to the indicated values.When adapting the absorption coefficient data to the temperature conditions of Jupiter, it is necessary to account for temperature corrections at temperate, tropical latitudes, and in the equatorial zone (EZ). This is due to the fact that the temperature structure of the atmosphere varies with latitude and altitude, which in turn affects the observed absorption. The laboratory spectrum of the methane absorption band at 890 nm is presented in the paper by O'Brien and Cao (2002) (O'Brien & Cao 2002). In the same paper, based on the Karkoschka data, numerical tabulated values of the absorption coefficient of methane in the range of 848.6–920.5 nm with a step of 1 at a temperature of 77 K are presented, which is an important source of data for various calculations related to the absorption band at 890 nm (Karkoschka 1994). The availability of such detailed spectral data allows for more accurate modeling of radiative transfer processes in the atmosphere. This paper also presents data on the absorption band of methane at 861 nm. The synthetic spectrum of the methane band at 890 nm is also presented in the paper by Fink, Benner and Dick (1977) (Fink et al. 1977). The spectrum is given with a resolution of 10 . This allows it to be used for comparative analysis with observational spectra and for refining the parameters of atmospheric models.

According to Fink et al., the methane absorption band at 890 nm occupies a wavelength range of 872.5–923.5 nm (Fink et al. 1977). Giver reported the range of this band

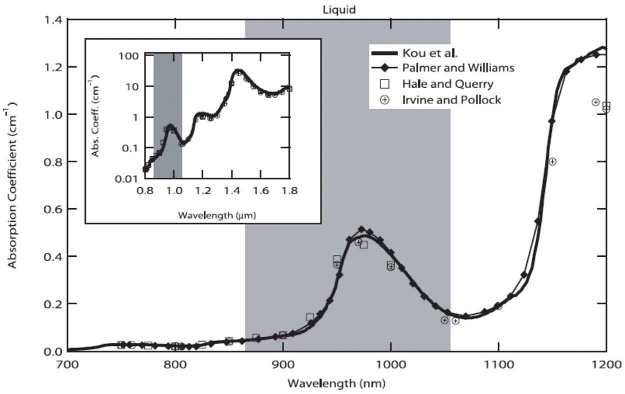

Figure 4. Near infrared water vapor absorption profile. The wavelength range used in this work is shown by the shaded area (Daniel et al. 2002).

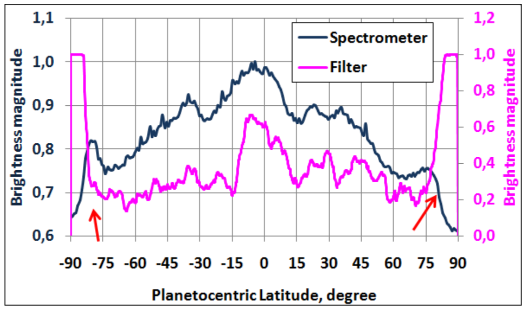

Figure 5. Comparison of brightness profiles of Jupiter's central meridian in the 890 nm band (see text for details).

to be 872.8–928.3 nm (Giver 1978). Minor differences in the reported ranges may be due to differences in measurement methods and criteria for determining band boundaries.

The accuracy of ground-based observations in the 890 nm band is virtually unaffected by water vapor in the Earth's atmosphere. This is confirmed by data published by (Daniel et al. 2002) which,presents the distribution of water vapor absorption. As can be seen from Figure 4, in the 890–905 nm region, there is only minor water vapor absorption with a gradual increase in the longer wavelength part of the spectrum. This makes this spectral region particularly favorable for ground-based observations of Jupiter's atmosphere. Similar results are presented in a report by the Max Planck Institute (Bartsch et al. 1997), which shows virtually zero absorption in the region of the methane absorption band at 890 nm, followed by an increase in the near-infrared region. This further confirms the high suitability of this spectral region for astronomical observations.

Observations of Jupiter using the 890 nm filter make it possible to identify features in its atmosphere that are not distinguishable at other wavelengths (Minton 1972; Moreno et al. 1991; Morales-Juberías et al. 2002; Sanchez-Lavega et al. 1998; Hueso et al. 2017). This is due to the fact that strong absorption of methane limits the contribution of deeper layers of the atmosphere and enhances the contrast of high-lying cloud structures. A characteristic feature of Jupiter is the presence of bright polar regions in the 890 nm band (see Figure 2). Figure 5 shows a comparison of photometric profiles of Jupiter's disk along the central meridian, obtained using the SBIG SGS spectrometer at a wavelength of 890 nm (Almaty, Kazakhstan, November 3, 2023, during opposition) and using the 889 nm filter on the Hubble Space Telescope (May 22, 2022) (Wong et al. 2023).

Red arrows indicate increased brightness in the polar regions. This increased brightness can be explained by the presence of high-altitude aerosol haze, likely caused by cosmic dust precipitation near the planet's magnetic poles. This phenomenon indicates active interactions between Jupiter's magnetosphere and atmosphere.

4 ANTICYCLONIC FORMATIONS AND THE GREAT RED SPOT (GRS)

Anticyclonic formations are observed at Jupiter's temperate and equatorial latitudes, appearing as highly bright in images in the 890 nm methane band. This intensity of reflected light can be explained either by an increased aerosol density in cloud structures or by a reduced thickness of the purely gaseous layer above the cloud top. According to Pérez-Hoyos et al. (2012), in the temperate latitudes of the southern hemisphere in 2009, the optical thickness of the above-cloud atmosphere was 0.2–0.9 (Pérez-Hoyos et al. 2012a), while according to Satoh & Kawabata, it did not exceed 0.32 (Satoh & Kawabata 1992). It should be noted that the studies by Pérez-Hoyos et al. took into account the impact of the collision with Comet Shoemaker–Levy. In addition to the given values, for some models Pérez-Hoyos et al. obtained an optical thickness of up to 1.3, which is associated with the consideration of deeper layers of the atmosphere (Pérez-Hoyos et al. 2012b).

Observations in the 890 nm band make it possible to detect haze above the cloud layer and compare it with data in the ultraviolet range of 410 nm (Banfield et al. 1998) and 325–375 nm (Owen & Mason 1969). However, strong variations at these wavelengths are masked by methane absorption (890 nm), aerosol absorption (410 nm), and Rayleigh scattering (325–375 nm), respectively.

The work of Satoh and Kawabata (1992) provides the parameters of atmospheric calculations and the results of modeling for the equatorial zone (EZ) and belts under various cloud models (Satoh & Kawabata 1992). In general, the values of the absorption coefficient are consistent with the data of O'Brien and Cao (O'Brien & Cao 2002). A number of other quantities characterizing the methane absorption band at 890 nm should also be taken into account.

According to Simon et al. the optical depth of the stratospheric haze layer in the 890 nm band is about 0.01, and the albedo of a single scattering of tropospheric haze at the same wavelength is 0.96 (Simon et al. 2015). Bardet et al. presented a map of brightness temperatures along the central meridian in the latitude range of ±70° for layers of 0.1 mbar–1 bar (Bardet et al. 2024). The map was constructed based on 281 observations made on May 24–27, 2018, using VISIR on the Very Large Telescope (VLT, Chile). Stratospheric tem-

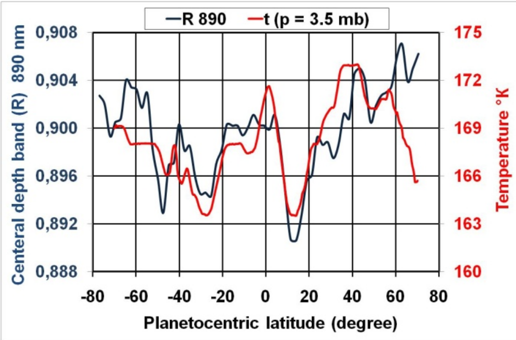

Figure 6. Central depth of the methane absorption band (890 nm) and Jovian brightness temperature at the 3.5 mbar pressure level between ±75° latitude.

perature was measured by methane emission at a wavelength of 7.9 μm. The observations covered the planet from pole to pole and were synchronized with the 13th perijove Juno mission, which allowed the comparison of ground-based infrared measurements with high-resolution Juno Cam images.

The use of 11 narrow-band filters in the range of 7.9–19.5 μm made it possible to reconstruct vertical profiles of temperature, NH_3, C_2H_2, C_2H_6 concentrations and aerosol characteristics using the nonlinear optimal estimation method (NEMESIS) Irwin et al., 2008 (Bardet et al. 2024).

Our spectral observations of Jupiter's central meridian showed a good correspondence between the meridional variation of the central depth of the 890 nm methane absorption band and the brightness temperature at a pressure level of 3.5 mbar (Bardet et al. 2024) on May 25, 2018, which will be presented and discussed in our next article.

The Great Red Spot (GRS) is a massive, cold-core anticyclonic structure surrounded by a warm cyclonic ring. The ring, known as a trough, has a high albedo. Anticyclonic circulation within the GRS, combined with interaction with the Jovian zonal wind system, can cause material from the trough to move into a triangular shape north of the GRS with an upper boundary at $\sim 15°$ S. Anticyclonic winds within the GRS gradually decay with height in the lower stratosphere. Cloud clearing within the cyclonic ring at 5 μm wavelength suggests that localized lifting within the GRS causes particle deposition at its periphery (Harkett et al. 2024).

Since methane is uniformly distributed in Jupiter's atmosphere, the 890 nm absorption band serves as a qualitative indicator of cloud-top pressure (Hill et al. 2024). Variations in the height of the atmospheric layer determined by the 890 nm methane band depend on the thermodynamic state of the stratosphere. The near infrared image of the vortex at 890 nm reveals a region of high aerosol reflectivity within the GRS (Harkett et al. 2024). The 890 nm band is sensitive to low pressures and is strongly influenced by high-level haze (Hill et al. 2024). Stratospheric haze absorption is stronger than tropospheric haze at wavelengths longer than 300 nm, since tropospheric haze exhibits relatively weak absorption in the visible range (Harkett et al. 2024). Consequently, tropospheric haze particles act as effective light scatterers (Fletcher 2020).

The 890 nm spectral region is dominated by CH_4 absorption at a level of ~ 100 mbar; such observations indicate that the bulk of the aerosol within the GRS is lifted to the upper troposphere or lower stratosphere (Harkett et al. 2024). Increasing the lower pressure of the stratospheric haze reduces the reflectivity in the 890 nm filter, since the light travels a longer path and is subject to greater absorption by methane (Anguiano-Arteaga et al. 2023). If we consider the coincidence of the latitudinal variation of temperature and the distribution of methane absorption, it can be noted that the layer of the atmosphere with a pressure less than 10 mbar is sensitive to the 890 nm band.

For the core of the Great Red Spot, the optical thicknesses of the stratospheric and tropospheric haze ($\tau_{\text{stratum}} = 0.25$; $\tau_{\text{tropum}} = 3.85$) and the optical thickness of the lower cloud ($\tau_{\text{cloud}} = 13$) were adopted (Anguiano-Arteaga et al. 2023). In general, for Jupiter, optically thin layers ($\tau \sim 0.1$) above the main tropospheric cloud ($\tau \sim 10$) are considered (Anguiano-Arteaga et al. 2023). The most reliable calculation results are achieved with a variable imaginary refractive index $\lambda < 400$ nm, $\tau_{\text{chromophore}}(900\,\text{nm}) = 0.16 \pm 0.05$ for the GRS core and $\tau_{\text{chromophore}}(900\,\text{nm}) = 0.14 \pm 0.06$ for the South Tropical Zone (STrZ) (Anguiano-Arteaga et al. 2023). In all cases, the overlying haze and chromophore layers are taken into account. For comparison, in the single scattering cloud layer model the layer range is from ~ 780 mbar to ~ 900 mbar (Hill et al. 2024; Anguiano-Arteaga et al. 2023).

The most optimal model includes the following parameters: stratospheric haze with a base at about 110 mbar, $r_{\text{eff}} \approx 0.3\,\mu$m, $\tau \sim 1$, and optically thick tropospheric haze with a base at 500 mbar, average particle size of 0.5–6 μm, τ up to 25. Most of the light attenuation occurs at levels above 500 mbar (Irwin et al. 2025). Harkett et al. note that the characteristic of ammonia ice NH_3 is strongly dependent on particle size: smaller radii create sharper absorption, while larger ones create a broad absorption characteristic (Harkett et al. 2024).

5 DISCUSSION

The obtained results demonstrate the complex nature of the interaction of the 890 nm methane band with Jupiter's atmosphere. The observed correlation between the central absorption band depth and the brightness temperature at levels of 3.5–8.6 mbar indicates that variations in the aerosol optical depth in this spectral range are largely controlled by the thermal structure of the atmosphere.

The Great Red Spot region deserves special attention, as the largest discrepancies between the temperature and methane absorption distributions were detected. This highlights the need to account for the unique dynamic structure of the GRS, including vertical and horizontal temperature gradients, updrafts and downdrafts, and local variations in aerosol concentration.

A comparison of ground-based observations (VLT/VISIR) and Juno mission results shows that the GRS is a deep baroclinic structure with a vertical extension from cloud tops to hundreds of kilometers into the atmosphere. This structure has a significant influence on stratospheric dynamics, is supported by a system of zonal jets, and exhibits a stable radiative-dynamical balance.

Overall, the data confirm that the 890 nm methane absorption band is a sensitive tool for studying the upper troposphere and lower stratosphere. The use of multiparameter models, including variations in optical depth, cloud height, and aerosol concentration, allows for a more accurate interpretation of the observed photometric and spectroscopic characteristics.

6 CONCLUSIONS

1 Observations in the 890 nm methane absorption band provide a highly effective method for diagnosing Jupiter's stratospheric haze and upper troposphere, with sensitivity to pressure levels from ~ 5 to 200 mbar.

2 Spectrophotometric measurements of the central depth of the 890 nm band revealed a stable correlation with the brightness temperature of the atmosphere at levels of 3.5–8.6 mbar, which indicates a close relationship between the thermal state and optical properties of the aerosol layer.

3 The largest deviations from the general absorption-temperature relationship are found in the region of the Great Red Spot, which is due to its complex vertical structure and dynamics, requiring the use of multi-layer atmospheric models for interpretation.

4 To further deepen our understanding of the physics of Jupiter's atmosphere, we need joint observational campaigns combining spectrophotometric and filter methods with high spatial resolution, as well as their comparison with data from space missions (Juno, JWST).

The work is carried out within the framework of the Project No. BR31714731 “Fundamental research in observational and theoretical astrophysics”, financed by the Ministry of Science and Higher Education of the Republic of Kazakhstan.

CONFLICT OF INTEREST

The authors declare that they have no conflict of interest.

REFERENCES

Morales-Juberías R., Sánchez-Lavega A., Dowling TE, Icar. 2003. V. **166**. No. 1. P. 63–74.
Banfield D., Gierasch PJ, Bell M., et al., Icar. 1998. V. **135**. No. 1. P. 230–250.
West RA, Strobel DF, Tomasko MG, Icar. 1986. V. **65**. No. 2–3. P. 161–217.
Bellini B., Bellucci G., Formisano V., P&SS. 1998. V. **46**. No. 9–10. P. 1305–1314.
Hill S., Adcock B., Cidadão A., et al., // Proceedings of the 42nd Annual Conference of the Society for Astronomical Sciences. 2023. P. 11–21.
Wong MH, Bjoraker GL, Goullaud C, et al., RemS. 2023. V. **15**. P. 702.
Atai A., Vdovichenko VD, Humbatova EE, et al., AzAJ, 2022, **17**, 1.
Vdovichenko VD, Kirienko GA, Lysenko PG, Proceedings of the National Academy Sciences. The Republic of Kazakhstan. Phys-math. Series, 2017, **4**, 204.
Teifel VG, et al., Proceedings of the National Academy of Sciences. The Republic of Kazakhstan. Phys-math. Series, 2017, **4**, 185.
Vdovichenko VD, Kirienko GA, Lysenko PG, Proceedings of the National Academy Sciences. The Republic of Kazakhstan. Phys-math. Series, 2016, **5**, 111.
Vdovichenko VD, et al., Proceedings of the National Academy of Sciences. The Republic of Kazakhstan. Phys-math. Series, 2014, **4**, 77.
Vdovichenko VD, et al., Proceedings of the National Academy of Sciences. The Republic of Kazakhstan. Phys-math. Series, 2015, **5**, 91.
Teifel VG, et al., Proceedings of the National Academy of Sciences. The Republic of Kazakhstan. Phys-math. series. 2018, **3**, 23.
Owen T., Mason HP, JAtS. 1969. V. **26**. No. 5. P. 870–873.
Karkoschka E., Icar. 1994. V. **111**. No. 1. P. 174–192.
O'Brien JJ, Cao H., JQSRT. 2002. V. **75**. No. 3. P. 323–350.
Fink U., Benner DC, Dick KA, JQSRT. 1977. V. **18**. No. 4. P. 447–457.
Giver LP, JQSRT. 1978. V. **19**. No. 3. P. 311–322.
Daniel JS, Solomon S, Portmann RW, et al., J.G.R. 2002. V. **107**. No. D21. pp. 4599–4615.
Bartsch B., Bakan S., Ehret G., et al., AdSR. 1997. **18**(7), 25–28.
Minton, R. B., CoLPL. 1972. **9**. 160–183.
Moreno F., Molina A., Lara LM, JGRA. 1991. V. **96**. No. A8. P. 14119–14127.
Morales-Juberías R., Sanchez-Lavega A., Colas F., Icar. 2002. V. **157**. No. 1. P. 76–90.
Sanchez - Lavega A., Hueso R., Acarreta JR, GeoRL. 1998. V. **25**. No. 21. P. 4043–4046.
Hueso R., Sánchez-Lavega A., Iñurrigarro P., et al., GeoRL. 2017. V. **44**. No. 10. P. 4669–4678.
Pérez-Hoyos S., Sanz-Requena JF, Sánchez-Lavega A., et al., Icar. 2012. V. **221**. No. 2. P. 1061–1078.
Satoh T., Kawabata K., ApJ. 1992. V. **384**. P. 298–304.
Pérez-Hoyos S., Sanz-Requena JF, Barrado-Izagirre N., et al., Icar. 2012. V. **217**. No. 1. P. 256–271.
Simon A. A., Sanchez-Lavega A., Legarreta J., et al., JGRE. 2015. V. **120**. No. 3. P. 483–494.
Bardet D., Donnelly PT, Fletcher LN, et al., JGRE. 2024. V. **129**. e2023JE007902.
Fletcher LN, Orton GS, Greathouse TK, et al., JGRE. 2020. V. **125**. e2020JE006399.
Fletcher L., Zenodo. 2020. doi: 10.5281/zenodo.3706793.
Harkett J, Fletcher LN, King ORT, et al., JGRE. 2024. V. **129**. e2024JE008415.
Hill SM, Irwin PGJ, Alexander C, Rogers JH, E&SS. 2024. V. **11**. e2024EA003562.
Anguiano-Arteaga A., Pérez-Hoyos S., Sánchez-Lavega A., et al., JGRE. 2023. V. **128**. e2022JE007427.
Irwin P. G. J, Hill SM, Fletcher LN, et al., JGRE. 2025. V. **130**. e2024JE008622.